Vectorial Electron Relay at ITO Electrodes Modified with Self-Assembled Monolayers of Ferrocene–Porphyrin–Fullerene Triads and Porphyrin–Fullerene Dyads for Molecular Photovoltaic Devices

Hiroshi Imahori,*[a] Makoto Kimura,[b] Kohei Hosomizu,[a] Tomoo Sato,[c] Tae Kyu Ahn,[d, e] Seong Keun Kim,[e] Dongho Kim,*[d] Yoshinobu Nishimura,[c] Iwao Yamazaki,*[f] Yasuyuki Araki,[g] Osamu Ito,*[g] and Shunichi Fukuzumi*[b]

Abstract: Systematic series of indium tin oxide (ITO) electrodes modified covalently with self-assembled monolayers (SAMs) of ferrocene–porphyrin–fullerene triads and porphyrin–fullerene dyads were designed to gain valuable insight into the development of molecular photovoltaic devices. The structures of SAMs on ITO have been investigated by UV/Vis absorption spectroscopy, atomic force microscopy, and cyclic voltammetry. The photoelectrochemical and photophysical (fluorescence lifetime and time-resolved transient absorption) properties were also determined. The highest quantum yield of photocurrent generation (11%) among donor–acceptor linked systems which are covalently attached to the surface of ITO electrodes was achieved with SAMs of ferrocene–zinc porphyrin–fullerene linked triad on ITO electrodes. The quantum yields of photocurrent generation correlate well with the charge-separation efficiency and the lifetime of the charge-separated state of the porphyrin–fullerene linked systems in solution. These results provide valuable information for the construction of photonic molecular devices and artificial photosynthetic systems on ITO electrodes.

Keywords: donor–acceptor systems · electron transfer · fullerenes · porphyrins · self-assembly

[a] Prof. Dr. H. Imahori, K. Hosomizu
Department of Molecular Engineering
Graduate School of Engineering, Kyoto University
PRESTO, Japan Science and Technology Agency (JST)
Nishikyo-ku, Kyoto 615-8510 (Japan)
and Fukui Institute for Fundamental Chemistry
Kyoto University, 34-4, Takano-Nishihiraki-cho
Sakyo-ku, Kyoto 606-8103 (Japan)
Fax: (+81) 75-383-2571
E-mail: imahori@scl.kyoto-u.ac.jp

[b] M. Kimura, Prof. Dr. S. Fukuzumi
Department of Material and Life Science
Graduate School of Engineering, Osaka University
CREST, Japan Science and Technology Agency (JST)
Suita, Osaka 565-0871 (Japan)
Fax: (+81) 6-6879-7370
E-mail: fukuzumi@chem.eng.osaka-u.ac.jp

[c] Dr. T. Sato, Dr. Y. Nishimura
Department of Chemistry, University of Tsukuba
Tsukuba, Ibaraki 305-8577 (Japan)

[d] T. K. Ahn, Prof. Dr. D. Kim
Center for Ultrafast Optical Characteristics Control
Department of Chemistry
Yonsei University, Seoul 120-749 (Korea)
Fax: (+82) 2-2123-2436
E-mail: dongho@yonsei.ac.kr

[e] T. K. Ahn, Prof. Dr. S. K. Kim
School of Chemistry, Seoul National University
Seoul 151-747 (Korea)

[f] Prof. Dr. I. Yamazaki
Department of Molecular Chemistry
Graduate School of Engineering
Hokkaido University, Sapporo 060-8628 (Japan)
Fax: (+81) 11-709-2037
E-mail: yamiw@eng.hokudai.ac.jp

[g] Dr. Y. Araki, Prof. Dr. O. Ito
Institute for Multidisciplinary Research for Advanced Materials
Tohoku University, CREST
Japan Science and Technology Agency (JST)
Sendai 980-8577 (Japan)
Fax: (+81) 22-217-5608
E-mail: ito@tagen.tohoku.ac.jp

Supporting information for this article is available on the WWW under http://www.chemeurj.org/ or from the author. UV/Vis absorption spectra of porphyrin-fullerene dyads on ITO and in solution (S1), fluorescence spectra of porphyrin–fullerene dyads on ITO and in solution (S2), AFM cross-section of porphyrin–fullerene linked systems on ITO (S3), concentration dependence of photocurrent generation on AsA for a ferrocene–porphyrin–fullerene triad system (S4), photoelectrochemical response of a porphyrin–fullerene dyad system (S5), fluorescence decay curve of a porphyrin–fullerene dyad on ITO (S6), and time profile of absorbance for a porphyrin–fullerene dyad on ITO (S7).

 DOI: 10.1002/chem.200400377

Introduction

Understanding photoinduced electron transfer (ET) in donor (D)–acceptor (A) linked systems under well-defined conditions is essential for the rational design and development of photovoltaic devices, photonic devices, photocatalysis, and artificial photosynthesis.[1] In this context coupling of a porphyrin donor and a fullerene acceptor has emerged rapidly in D–A linked systems, since the D–A couples exhibit excellent ET properties owing to small reorganization energies as compared to conventional aromatic D–A systems.[2,3] For example, in porphyrin–fullerene linked dyads photoinduced ET from the porphyrin excited singlet state to the C_{60} moiety occurs nearly at the top region of the Marcus parabolic curve, whereas the charge-recombination process is shifted deeply into the inverted region of the Marcus parabolic curve, which is a key strategy for efficient ET in photosynthesis. Thus, photoexcitation leads to the formation of a long-lived charge-separated state with a high quantum yield in solution by photoinduced ET. This methodology has allowed us to construct a variety of porphyrin–fullerene linked systems which exhibit efficient charge separation (CS) and slow charge recombination (CR).[2] However, the structures and photophysical properties of D–A linked systems in solution are in a sharp contrast with those in molecular assemblies, where the intermolecular interaction and surrounding environment significantly influence their properties. Thus, research on D–A linked systems in molecular assemblies is of utmost importance to gain further insight into their photophysical and photochemical applications.

Self-assembled monolayers (SAMs) are highly promising for constructing molecular architectures on metal and semiconductor surfaces.[4] Self-assembled monolayers of photoactive chromophores on flat gold surfaces have attracted special attention as photonic molecular devices and artificial photosynthetic materials.[5–17] In particular, donor–acceptor linked molecules or mixtures of donor–acceptor components self-assembled on gold electrodes exhibit photosynthetic ET and energy transfer (EN), and generate a photocurrent as macroscopic output.[7,8,11,16,17] However, a high quantum yield for photocurrent generation on the electrode, as attained in photosynthesis, has been hampered by strong EN quenching of the excited states of chromophores by the gold surface.[11c] Indium tin oxide (ITO) with high optical transparency and electrical conductivity seems to be a promising alternative as an electrode which may reduce the quenching of the excited states of chromophores on the surface. Despite these advantages, development of SAMs on ITO electrodes has been restricted because their chemical modification requires carefully controlled conditions which are difficult to achieve.[18] As such, the synthetic approach to SAMs on gold electrodes is not applicable to SAMs on ITO, which has hydroxyl groups on the surface and exhibits high roughness as opposed to the atomically flat Au(111) surface. Thus, no systematic studies on the structures and photophysical properties of SAMs of donor–acceptor linked molecules on ITO have hitherto been reported.[19–25]

We report herein a series of SAMs of porphyrin–fullerene linked triads and dyads on ITO electrodes designed to study this issue. Ferrocene–porphyrin–fullerene triads and porphyrin–fullerene dyads were selected as donor–acceptor linked systems because of their pronounced CS in solution. The investigated systems are shown in Schemes 1 and 2. The series are SAMs of ferrocene–porphyrin (P)–C_{60} triads on ITO electrodes [denoted as **Fc-P-CONH-C_{60}**/ITO (P = ZnP or H_2P)], SAMs of P–C_{60} dyads with a diphenylamido spacer on ITO electrodes [denoted as **P-CONH-C_{60}**/ITO (P = ZnP or H_2P)], SAMs of P–C_{60} dyads with a phenyl spacer on ITO electrodes [denoted as **P-S1-C_{60}**/ITO (P = ZnP or H_2P)], a C_{60} SAM without porphyrin [denoted as **C_{60}-ref**/ITO],[26] and porphyrin SAMs without C_{60} [denoted as **P-ref**/ITO (P = ZnP or H_2P)].[27] The photoelectrochemical and photophysical (fluorescence lifetime and time-resolved transient absorption) properties of the ITO systems were examined. Their photodynamic properties are compared with those of ferrocene–porphyrin–fullerene triads [**Fc-P-CONH-C_{60}** (P = ZnP or H_2P)][28c] and porphyrin–fullerene dyads (**P-CONH-C_{60}** (P = ZnP or H_2P)[28] and **P-S1-C_{60}** (P = ZnP or H_2P)[29]) in solution. The surface structures were investigated by atomic force microscopy (AFM). The photoelectrochemical properties were also compared with those of a SAM of porphyrin–fullerene dyad in which the chromophores are arranged in reverse direction on ITO [denoted as **C_{60}-NHCO-P**/ITO (P = ZnP)[27]]. Thus, the present study provides the first comprehensive data on a series of ITO electrodes modified with SAMs of porphyrin–fullerene dyads and ferrocene–porphyrin–fullerene triads.

Results and Discussion

Preparation: The general strategy employed for the synthesis of SAMs is summarized in Scheme 3. The ITO electrodes [ca. 100 nm ITO on transparent glass slides (Evers, Inc., Japan)] were treated with (3-aminopropyl)trimethoxysilane by refluxing in toluene under N_2. The aminopropylsilylated ITO electrode was then immersed in a 1 mmol L^{-1} toluene solution of C_{60} for two days under reflux to give **C_{60}-ref**/ITO.[26] Porphyrin aldehydes **1**–**3**[28b,29,30] were coupled to **C_{60}-ref**/ITO by refluxing in the presence of *N*-methylglycine for three days in toluene to give **Fc-P-CONH-C_{60}**/ITO (P = ZnP or H_2P), **P-CONH-C_{60}**/ITO (P = ZnP or H_2P), and **P-S1-C_{60}**/ITO (P = ZnP or H_2P), respectively.[31] The 1,3-dipolar cycloaddition of azomethine ylides to C_{60} affording fulleropyrolidines occurs exclusively across [6,6] bonds.[31] One would expect different proportions of isomeric bis-adducts on the ITO surface due to the less chemoselective Prato bis-addition. However, *trans*-1,2,3,4 positions relative to the [6,6] bond undergoing the first addition may be preferable for the second addition because of the steric hindrance around a C_{60} moiety self-assembled on the ITO surface.[32,33] Porphyrin SAMs on ITO electrodes [**P-ref**/ITO (P = ZnP or H_2P)],[27] ferrocene–porphyrin–fullerene triads [**Fc-P-CONH-C_{60}** (P = ZnP or H_2P)[28c]], and porphyrin–fullerene dyads [**P-CONH-C_{60}** (P = ZnP or H_2P)[28] and **P-S1-C_{60}** (P = ZnP or H_2P)[29]] were obtained by following the same procedures as described previously. Structures of all new compounds were confirmed by spectroscopic analysis including

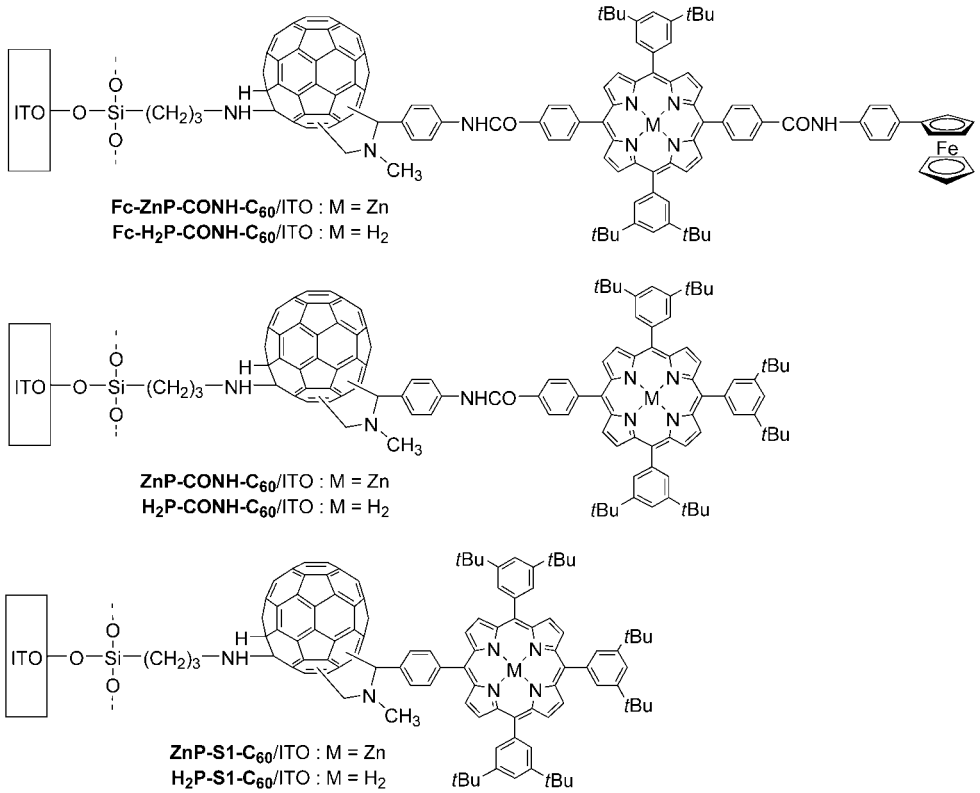

Scheme 1. Self-assembled monolayers of ferrocene–porphyrin–fullerene triads and porphyrin–fullerene dyads on ITO.

^{1}H NMR and MALDI-TOF mass spectra (see Experimental Section).

Spectroscopic and electrochemical studies and surface characterization: Figure 1 displays the absorption spectra of **Fc-ZnP-CONH-C$_{60}$**/ITO and reference **Fc-ZnP-CONH-C$_{60}$** in THF. The Soret band of **Fc-ZnP-CONH-C$_{60}$**/ITO is broader than that of **Fc-ZnP-CONH-C$_{60}$** in THF. The λ_{max} value of the Soret band of **Fc-ZnP-CONH-C$_{60}$**/ITO (435 nm) is red-shifted by 9 nm relative to that of **Fc-ZnP-CONH-C$_{60}$** in THF (426 nm[16d]). The peak position of the Q band of **Fc-ZnP-CONH-C$_{60}$**/ITO is also red-shifted relative to that of **Fc-ZnP-CONH-C$_{60}$** in THF. Similar red shifts and broadening of the Soret band were observed for **Fc-H$_2$P-CONH-C$_{60}$**/ITO (8 nm), **ZnP-CONH-C$_{60}$**/ITO (6 nm), **H$_2$P-CONH-C$_{60}$**/ITO (4 nm), **ZnP-S1-C$_{60}$**/ITO (5 nm), and **H$_2$P-S1-C$_{60}$**/ITO (4 nm) relative to **Fc-H$_2$P-CONH-C$_{60}$**, **ZnP-CONH-C$_{60}$**, **H$_2$P-CONH-C$_{60}$**, **ZnP-S1-C$_{60}$**, and **H$_2$P-S1-C$_{60}$** in THF (see Supporting Information S1). The λ_{max} values of the Soret bands, listed in Table 1, indicate that the porphyrin environments on ITO are similar and perturbed moderately within the monolayers, as compared to the reference systems in THF, due to aggregation.[11c] Fluorescence spectra of **Fc-P-CONH-C$_{60}$**/ITO (P = ZnP or H$_2$P), **P-CONH-C$_{60}$**/ITO (P = ZnP or H$_2$P), and **P-S1-C$_{60}$**/ITO (P = ZnP or H$_2$P) were recorded by photoexcitation at 420 nm for free-base porphyrins and 427 nm for zinc porphyrins (see Supporting Information S2). For example, the emission maxima of **Fc-ZnP-CONH-C$_{60}$**/ITO (611, 657 nm) are red-shifted by 5–6 nm relative to **Fc-ZnP-CONH-C$_{60}$** in THF (605, 652 nm[16d]). Similar behavior is seen for **Fc-H$_2$P-CONH-C$_{60}$**/ITO, **ZnP-CONH-C$_{60}$**/ITO, **H$_2$P-CONH-C$_{60}$**/ITO, **ZnP-S1-C$_{60}$**/ITO, and **H$_2$P-S1-C$_{60}$**/ITO. This also suggests that the porphyrin environments on ITO are perturbed moderately within the monolayers due to aggregation.[34]

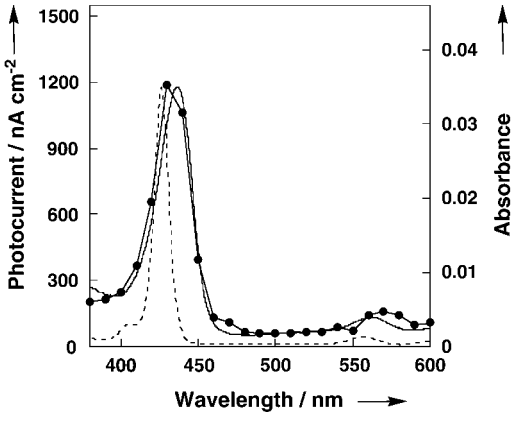

Figure 1. UV/Vis absorption spectra of **Fc-ZnP-CONH-C$_{60}$**/ITO (solid line), **Fc-ZnP-CONH-C$_{60}$** in THF (dashed line), and action spectrum of ITO/**Fc-ZnP-CONH-C$_{60}$**/AsA/Pt system (solid line with filled circles); input power: 500 μW cm^{-2}; applied potential: +0.15 V versus Ag/AgCl (saturated KCl); argon-saturated 0.1 mol L^{-1} aqueous solution of Na_2SO_4 containing 50 mmol L^{-1} AsA. The spectra are normalized at the Soret band for comparison.

Cyclic voltammetry measurements on **Fc-P-CONH-C$_{60}$**/ITO, **P-CONH-C$_{60}$**/ITO, **P-S1-C$_{60}$**/ITO, **C$_{60}$-ref**/ITO, **Fc-P-CONH-C$_{60}$**, **P-CONH-C$_{60}$**, and **P-S1-C$_{60}$** (P = ZnP or H$_2$P) in

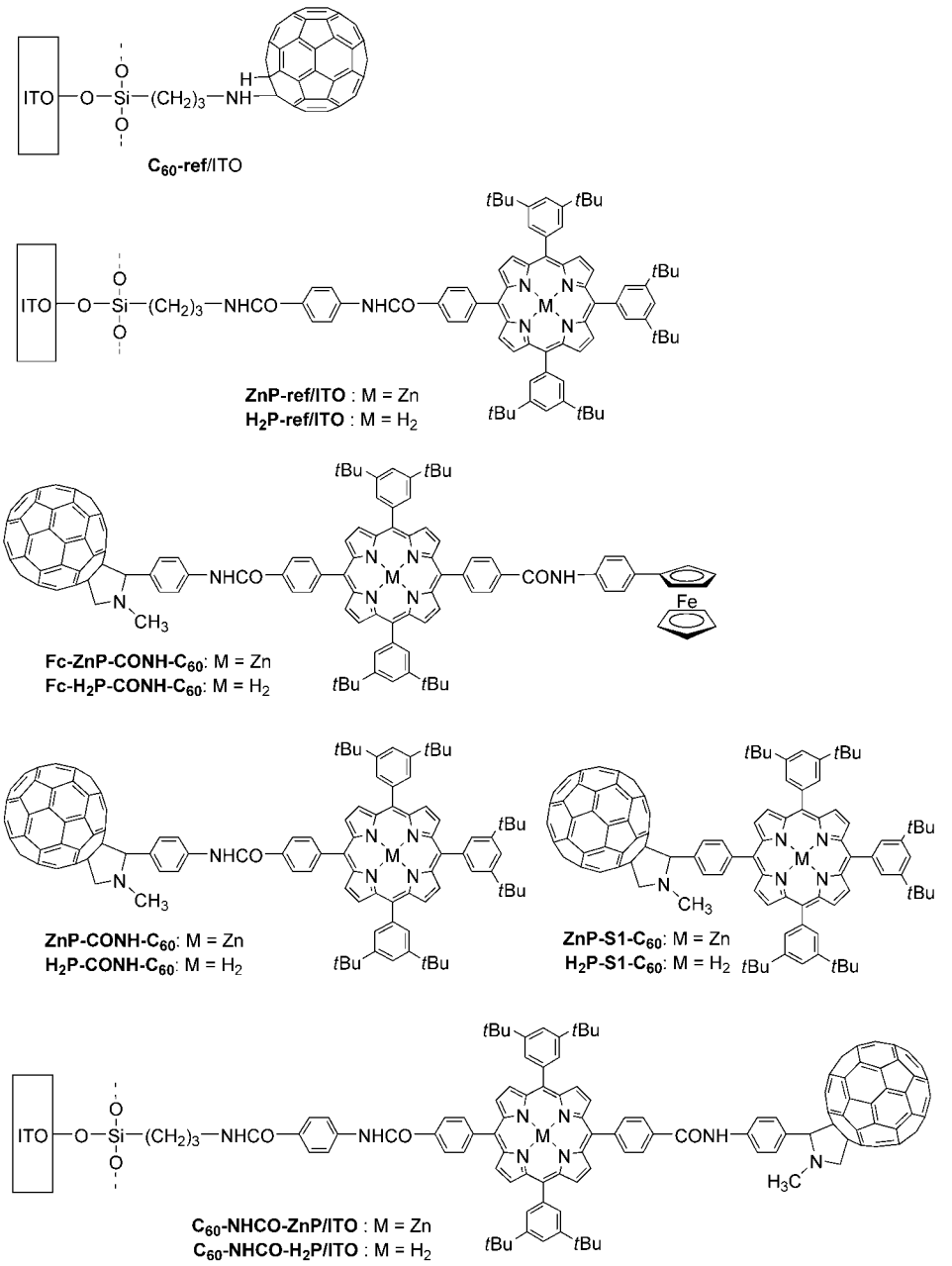

Scheme 2. Self-assembled monolayers of porphyrin and fullerene references and porphyrin–fullerene dyads on ITO and porphyrin–fullerene references used in this study.

CH_2Cl_2 containing 0.2 mol L^{-1} nBu$_4$NPF$_6$ were performed with a sweep rate of 0.10 V s^{-1} (electrode area 0.48 cm^{-2}) to estimate the surface coverage (Figure 2 and Table 1). For instance, the cyclic voltammogram of **C_{60}-ref**/ITO is characterized by a cathodic wave showing a well-defined current maximum, but by a small anodic wave on the reverse scan at 0.10 V s^{-1} [−0.69 V versus Ag/AgCl (saturated KCl)] due to the instability of the radical anion (Figure 2a). The linear increase of the anodic current with increasing scan rate implies that the fullerene is a surface-confined electroactive molecule. The adsorbed amount Γ of C_{60} on **C_{60}-ref**/ITO were calculated from the first cathodic peak current of C_{60} as 2.0×10^{-10} mol cm^{-2} (83 Å^2 molecule^{-1}) by using the roughness factor of 1.3 for ITO electrodes from atomic force microscopy (vide infra). This value is in a good agreement with the well-packed surface coverage of C_{60} SAM on ITO and gold electrodes [$(1.9–2.0)\times10^{-10}$ mol cm^{-2}],[7,26] although the modified ITO surface is not atomically smooth due to rather complex surface modification with the silane-coupling reagent and the intrinsically rough surface (ca. 50 nm). On the other hand, the cyclic voltammogram of **Fc-ZnP-CONH-C_{60}**/ITO exhibits a reversible oxidation wave due to the first oxidation of the zinc porphyrin moiety [0.88 V versus Ag/AgCl (saturated KCl)] and the first oxidation of the ferrocene moiety [0.56 V versus Ag/AgCl (saturated KCl)], as shown in Figure 2b.[35,36] Similar oxidation behavior due to the first oxidation of the porphyrin and ferrocene moieties is noted for **Fc-H$_2$P-CONH-C_{60}**/ITO (Figure 2c), **ZnP-CONH-C_{60}**/ITO, **H$_2$P-CONH-C_{60}**/ITO, **ZnP-S1-C_{60}**/ITO, and **H$_2$P-S1-C_{60}**/ITO. The first oxidation potentials of the porphyrin moieties for **Fc-ZnP-CONH-C_{60}** and **Fc-H$_2$P-CONH-C_{60}** in CH_2Cl_2 were reported to be $E^0_{ox}=0.86$ and 1.02 V versus Ag/AgCl (saturated KCl),[16d] which are virtually the same as those of **Fc-ZnP-CONH-C_{60}**/ITO (0.88 V versus Ag/AgCl) and **Fc-H$_2$P-CONH-C_{60}**/ITO (1.08 V versus Ag/AgCl).[37] Similar matching is noted for the first oxidation potentials of the ferrocene moieties for **Fc-P-CONH-C_{60}**/ITO and **Fc-P-CONH-C_{60}** in CH_2Cl_2 (P = ZnP or H$_2$P). The adsorbed amounts Γ of porphyrin on **Fc-ZnP-CONH-C_{60}**/ITO and **Fc-H$_2$P-CONH-C_{60}**/ITO were calculated from the first anodic peak currents of the ferrocene moieties as 9.0×10^{-11} mol cm^{-2} (190 Å^2 molecule^{-1}) and 9.3×10^{-11} mol cm^{-2} (180 Å^2 molecule^{-1}),[8c] respectively. The Γ values and redox potentials are listed in Table 1. The relative molar ratio of the ferrocene–porphyrin dyad and C_{60} moieties is about 1:2 for **Fc-ZnP-CONH-C_{60}**/ITO and **Fc-H$_2$P-CONH-C_{60}**/ITO. The occupied area per molecule of the ferrocene–porphyrin dyad moiety would vary depending on whether they are well-packed on the electrode surface in a parallel (ca. 800 Å^2 molecule^{-1}) or vertical (ca. 100 Å^2 molecule^{-1}) orientation to the surface plane. Since the relative molar ratio of

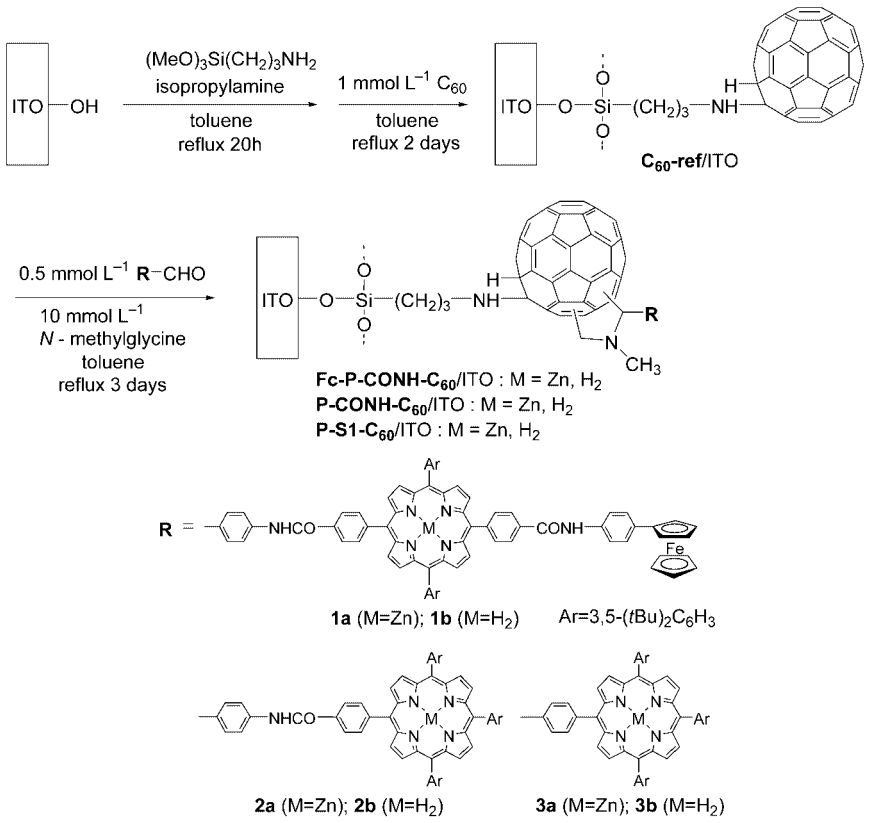

Scheme 3. General strategy employed for the synthesis of SAMs.

Table 1. Spectral data, redox potentials, and surface coverage.

System	Absorbance[a]	λ_{max} [nm][b]	Redox potential [V][c]		Γ [10^{-11} mol cm^{-2}][d]
			Fc/Fc^+	$P/P^{\cdot+}$	
Fc-ZnP-CONH-C_{60}/ITO	0.035	435	0.56	0.88	9.0
Fc-H_2P-CONH-C_{60}/ITO	0.037	428	0.57	1.08	9.3
ZnP-CONH-C_{60}/ITO	0.024	432		0.91	4.8
H_2P-CONH-C_{60}/ITO	0.028	424		1.08	5.3
ZnP-S1-C_{60}/ITO	0.012	431		0.91	4.6
H_2P-S1-C_{60}/ITO	0.015	424		1.06	5.1
ZnP-ref/ITO	0.030[e]	434		0.81	7.0
H_2P-ref/ITO	0.030[e]	426[e]		1.05[e]	14[e]
Fc-ZnP-CONH-C_{60}		426[f,g]	0.52[f]	0.86[f]	
Fc-H_2P-CONH-C_{60}		420[f,g]	0.56[f]	1.02[f]	
ZnP-CONH-C_{60}		426[f,g]		0.86[f]	
H_2P-CONH-C_{60}		420[f,g]		1.04[f]	
ZnP-S1-C_{60}		426[g]		0.87	
H_2P-S1-C_{60}		420[g]		1.04	

[a] Absorbance at the Soret band. [b] λ_{max} at the Soret band. [c] Measured in CH_2Cl_2 containing 0.2 mol L^{-1} nBu$_4$NPF$_6$ with a sweep rate of 0.1 V s^{-1} and Ag/AgCl (saturated KCl) as reference. [d] Obtained from the area of the anodic peak due to the first porphyrin oxidation by cyclic voltammetry. [e] From ref. [27]. [f] From ref. [16d]. [g] Measured in THF.

the ferrocene–porphyrin dyad to the C_{60} moiety is 1:2, the ferrocene-porphyrin dyad moiety may have a vertical orientation to the electrode surface rather than a parallel orientation. Such a packing structure is consistent with the UV/Vis and fluorescence spectroscopic data, which reveal considerable interactions between porphyrin moieties on ITO (vide infra).

To obtain further information on the surface structures of **Fc-ZnP-CONH-C_{60}**/ITO, **C_{60}-ref**/ITO, and ITO itself, we performed tapping-mode AFM measurements in air (NanoScope IIIa, Digital Instruments). The ITO surface exhibits its domain structures with a diameter of 50–100 nm and a height of about 50 nm (Figure 3a). After modification with C_{60}, the ITO surface reveals a similar image that indicates uniform coverage with C_{60} molecules (Figure 3b). However, the surface of **ZnP-CONH-C_{60}**/ITO exhibits additional small domain structures with a diameter of 20–40 nm and an average height of 3.1 nm, which corresponds to aggregates of the porphyrin moiety (Figure 3c and Supporting Information S3). The surface of **Fc-ZnP-CONH-C_{60}**/ITO also shows additional small domain structures with diameters of 20–40 nm and an average height of 3.9 nm, which correspond to aggregates of the ferrocene–porphyrin dyad moiety (Figure 3d). These results are consistent with the electrochemical data.

Photoelectrochemical measurements: Photoelectrochemical measurements were carried out in an argon-saturated 0.1 mol L^{-1} aqueous solution of Na_2SO_4 containing 50 mmol L^{-1} ascorbic acid (AsA) as an electron sacrificer with **Fc-P-CONH-C_{60}**/ITO (P = ZnP or H_2P), **P-CONH-C_{60}**/ITO (P = ZnP or H_2P), or **P-S1-C_{60}**/ITO (P = ZnP or H_2P) as working electrode, a platinum counterelectrode, and an Ag/AgCl (saturated KCl) reference electrode (hereafter represented by Pt/AsA/**Fc-P-CONH-C_{60}**/ITO, Pt/AsA/**P-CONH-C_{60}**/ITO, Pt/AsA/**P-S1-C_{60}**/ITO, respectively, where a slash denotes an interface). When **Fc-ZnP-CONH-C_{60}**/ITO electrode was irradiated with $\lambda = 430 \pm 5.0$ nm light with a power density of 500 μW cm^{-2} at an applied potential of +0.15 V versus Ag/AgCl (saturated KCl), a stable anodic photocurrent from the electrolyte to the ITO electrode appeared, as shown in Figure 4a. The photocurrent dropped instantly when the illumination was cut off. There is a good linear relationship between the photocurrent and the light intensity at each wavelength (from 0.10 to 6.0 mW cm^{-2}). In the absence of AsA, the anodic photocurrent was negligible under other-

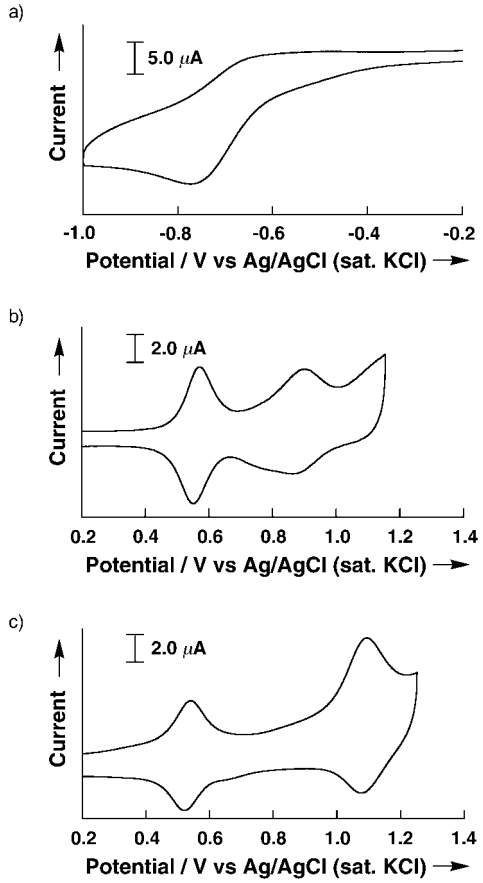

Figure 2. Cyclic voltammograms of a) **C_{60}-ref**/ITO, b) **Fc-ZnP-CONH-C_{60}**/ITO, and c) **Fc-H_2P-CONH-C_{60}**/ITO in CH_2Cl_2 containing 0.2 mol L^{-1} nBu$_4$NPF$_6$ at a sweep rate of 0.10 V s^{-1}; electrode area: 0.48 cm^2; counter-electrode: Pt wire; reference electrode: Ag/AgCl (saturated KCl).

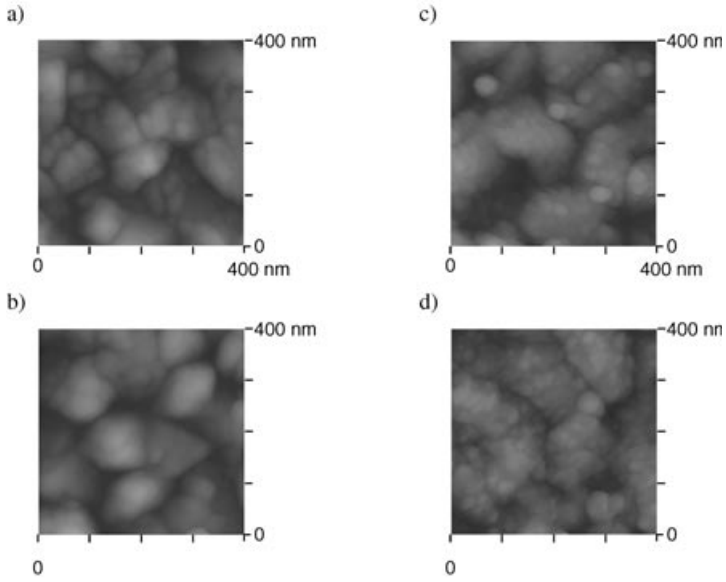

Figure 3. Tapping-mode atomic force micrographs of a) ITO (Z range: 50 nm), b) **C_{60}-ref**/ITO (Z range: 50 nm), and c) **ZnP-CONH-C_{60}**/ITO (Z range: 50 nm), d) **Fc-ZnP-CONH-C_{60}**/ITO (Z range: 50 nm) in air. The color scale represents the height topography, with bright and dark representing the highest and lowest features, respectively.

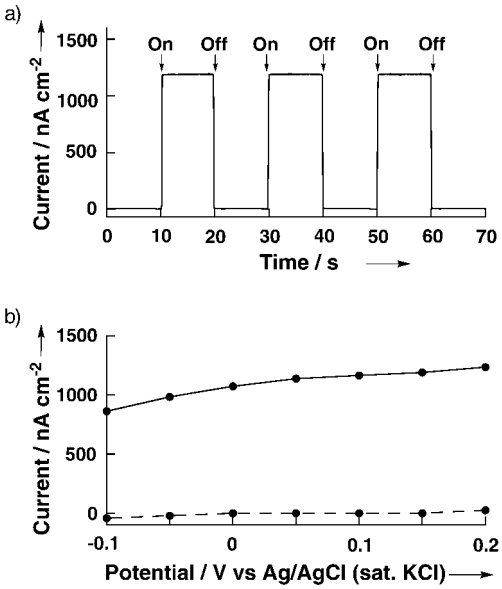

Figure 4. a) Photoelectrochemical response of Pt/AsA/**Fc-ZnP-CONH-C_{60}**/ITO; applied potential: +0.15 V versus Ag/AgCl (saturated KCl). b) Photocurrent versus applied potential curves for Pt/AsA/**Fc-ZnP-CONH-C_{60}**/ITO (solid line with filled circles). The dark current is shown as a dashed line with filled circles. $\lambda = 430 \pm 5.0$ nm (500 μW cm^{-2}); argon-saturated 0.1 mol L^{-1} aqueous solution of Na_2SO_4 containing 50 mmol L^{-1} AsA.

wise the same experimental conditions. Further addition of AsA (> 50 mmol L^{-1}) to the electrolyte solution did not increase the photocurrent significantly (see Supporting Information S4).[38] The anodic photocurrent increases monotonically with increasing positive bias to the ITO electrode [from −0.10 to +0.20 V versus Ag/AgCl (saturated KCl)], whereas the dark current remains constant, as shown in Figure 4b. The agreement of the action spectrum (filled circles in Figure 1) with the absorption spectrum of **Fc-ZnP-CONH-C_{60}**/ITO in 380–600 nm (solid line in Figure 1) demonstrates clearly that porphyrins are the photoactive species responsible for photocurrent generation and that the photocurrent flows from the electrolyte to the ITO electrode via the excited state of the porphyrin SAM.

Similar photoelectrochemical behavior was observed for the corresponding porphyrin–fullerene SAMs on the ITO electrode, denoted as Pt/AsA/**Fc-H_2P-CONH-C_{60}**/ITO, Pt/AsA/**ZnP-CONH-C_{60}**/ITO, Pt/AsA/**H_2P-CONH-C_{60}**/ITO, Pt/AsA/**ZnP-S1-C_{60}**/ITO, and Pt/AsA/**H_2P-S1-C_{60}**/ITO (see Supporting Information S5). The quantum yields of photocurrent generation were compared for Pt/AsA/**Fc-P-CONH-C_{60}**/ITO, Pt/AsA/**P-CONH-C_{60}**/ITO, and Pt/AsA/**P-S1-C_{60}**/ITO at an applied potential of +0.15 V versus Ag/AgCl (saturated KCl), for which the dark current is negligible. The quantum yields ϕ based on the number of photons absorbed by the chromophores were calculated from the input power ($\lambda = 419 \pm 5.3$ nm for free-base porphyrins and $\lambda = 430 \pm 5.0$ nm for zinc porphyrins, light intensity of 500 μW cm^{-2}), the photocurrent density, and the absorbance on the electrodes. The ϕ values decrease in the order of Pt/AsA/**Fc-ZnP-CONH-C_{60}**/ITO (11%), Pt/AsA/**ZnP-CONH-C_{60}**/ITO (8.0%), Pt/AsA/**H_2P-CONH-C_{60}**/ITO (5.1%), Pt/AsA/**Fc-**

H_2P-CONH-C_{60}/ITO (4.5%), Pt/AsA/**H_2P-S1-C_{60}**/ITO (3.4%), and Pt/AsA/**ZnP-S1-C_{60}**/ITO (1.7%), as summarized in Table 2. The ϕ value of Pt/AsA/**Fc-ZnP-CONH-C_{60}**/ITO system (11%) is the highest ever reported for photocurrent generation by using donor–acceptor linked molecules covalently tethered to an ITO surface.[27] The IPCE values of the present systems were also determined (Table 2). Despite the improved ϕ value, the IPCE value of Pt/AsA/**Fc-ZnP-CONH-C_{60}**/ITO system (0.7%) is still small because of the poor light-collecting property inherent to the monolayer system.

Table 2. Fluorescence lifetimes, quantum yields of charge separation and photocurrent generation, IPCE values, and lifetimes of charge-separated states.

System	Fluorescence lifetime τ [ns][a] (relative amplitude/%)	Quantum yield ϕ [%] (IPCE/%)	Lifetime τ [ns]
Fc-ZnP-CONH-C_{60}/ITO	0.053 (69), 0.21 (31)	11[f] (0.70[g])	
Fc-H_2P-CONH-C_{60}/ITO	0.30 (65), 1.1 (35)	4.5[f] (0.45[g])	
ZnP-CONH-C_{60}/ITO	0.053 (92), 0.42 (8)	8.0[f] (0.31[g])	
H_2P-CONH-C_{60}/ITO	0.31 (80), 1.2 (20)	5.1[f] (0.070[g])	
ZnP-S1-C_{60}/ITO	0.086 (79), 1.3 (21)	1.7[f] (0.026[g])	
H_2P-S1-C_{60}/ITO	0.16 (83), 1.1 (17)	3.4[f] (0.033[g])	
ZnP-ref/ITO	0.089 (77), 0.31 (23)[b]	0.38[b,f]	
H_2P-ref/ITO	1.2 (43), 4.6 (57)[b]	0.21[b,f]	
Fc-ZnP-CONH-C_{60}	0.095 (100)[c,d]	99[c,d]	7500[c,d]
Fc-H_2P-CONH-C_{60}	0.66 (100)[d]	25[c,d]	8300[c,d]
ZnP-CONH-C_{60}	0.10 (100)[c,d]	99[c,d]	770[c,d]
H_2P-CONH-C_{60}	1.3 (100)[d]	88[d]	45[c,d]
ZnP-S1-C_{60}	0.002 (100)[d,e]	18[d]	300[d]
H_2P-S1-C_{60}	0.027 (100)[d,e]	100[d,e]	0.91[d,e]

[a] Obtained by a single-photon counting technique for samples excited at 435 nm and monitored at 655 nm for free-base porphyrins and 605 nm for zinc porphyrins. [b] From ref. [27]. [c] From ref. [28c]. [d] In benzonitrile. [e] From ref. [29]. [f] Obtained in the standard three-electrode system. The quantum yields of photocurrent generation were obtained by the following equation: $\phi=(i/e)/[I(1-10^{-A})]$, where $I=W\lambda/hc$, i is the photocurrent density, e the elementary charge, I the number of photons per unit area and unit time, λ the wavelength of light irradiation, A the absorbance of the adsorbed dyes at λ, W the light power irradiated at λ, c the velocity of light, and h the Planck constant. [g] IPCE/% $=100\times1240\times i/(W\lambda)$, where W the incident light intensity [W] and λ the excitation wavelength [nm]. Argon-saturated 0.1 mol L^{-1} aqueous solution of Na_2SO_4 containing 50 mmol L^{-1} AsA; excitation with light at $\lambda=419\pm5.3$ nm for free-base porphyrins and $\lambda=430\pm5.0$ nm for zinc porphyrins with 500 μW cm^{-2} at a bias of +0.15 V versus Ag/AgCl (saturated KCl).

Fluorescence lifetime and transient absorption measurements: Remarkable differences in the quantum yields of photocurrent generation may stem from differences in the photophysical properties of **Fc-P-CONH-C_{60}**/ITO, **P-CONH-C_{60}**/ITO, and **P-S1-C_{60}**/ITO (P = ZnP or H_2P). Thus, we performed time-correlated, single-photon counting fluorescence measurements on **Fc-P-CONH-C_{60}**/ITO, **P-CONH-C_{60}**/ITO, and **P-S1-C_{60}**/ITO (P = ZnP or H_2P) to compare the fluorescence lifetimes with those reported for **P-ref**/ITO, **Fc-P-CONH-C_{60}**, **P-CONH-C_{60}**, and **P-S1-C_{60}** (P = ZnP or H_2P) in solution with photoexcitation at 435 nm. In each case the fluorescence decays of the excited singlet states of zinc porphyrin and free-base porphyrin (^{1}P*) were monitored at 605 and 655 nm, respectively. The decay curves can be well fitted by double exponentials, as shown in Figure 5, and the fluorescence lifetimes τ are summarized in Table 2. The weighted average fluorescence lifetimes of **Fc-ZnP-CONH-C_{60}**/ITO (0.10 ns), **ZnP-CONH-C_{60}**/ITO (0.082 ns), **Fc-H_2P-CONH-C_{60}**/ITO (0.58 ns), and **H_2P-CONH-C_{60}**/ITO (0.49 ns) are shorter than those of **ZnP-ref**/ITO (0.13 ns) and **H_2P-ref**/ITO (3.1 ns), respectively (see Supporting Information S6).[39,40] The weighted average fluorescence lifetime of **H_2P-S1-C_{60}**/ITO (0.32 ns) is also shorter than that of **H_2P-ref**/ITO.[40] This can be ascribed to the strong quenching of the porphyrin singlet excited states by the attached C_{60} moiety via intramolecular ET on the ITO surface. Note that the fluorescence lifetimes of the major components for **Fc-P-CONH-C_{60}**/ITO, **P-CONH-C_{60}**/ITO, and **P-S1-C_{60}**/ITO (P = ZnP or H_2P) are much shorter than those in THF, that is, ET rate constants in SAMs are larger than those in solution.[41]

The femtosecond time-resolved transient absorption spectrum of **Fc-ZnP-CONH-C_{60}**/ITO with photoexcitation at 400 nm was recorded to confirm photoinduced ET from the porphyrin excited singlet state to the C_{60} moiety on ITO. The decay of transient absorbance at 430 nm from the porphyrin excited singlet state is clearly observed (Figure 6). Unfortunately, however, the rise in absorbance due to the porphyrin radical cation could not be detected clearly because of the low signal-to-noise ratio. The temporal profile in Figure 6 can be fitted by a double exponential decay [50 ps (81%),

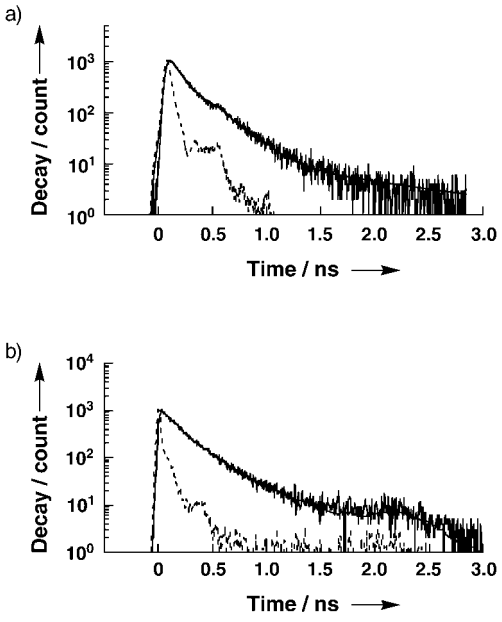

Figure 5. Fluorescence decay curves of a) **Fc-ZnP-CONH-C_{60}**/ITO and b) **ZnP-ref**/ITO observed at 605 nm by the single-photon counting method. The excitation wavelength was 435 nm.

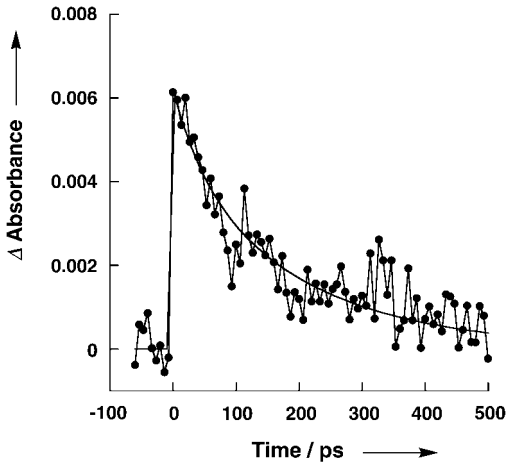

Figure 6. Time profile of **Fc-ZnP-CONH-C_{60}**/ITO at 430 nm after photoexcitation at 400 nm.

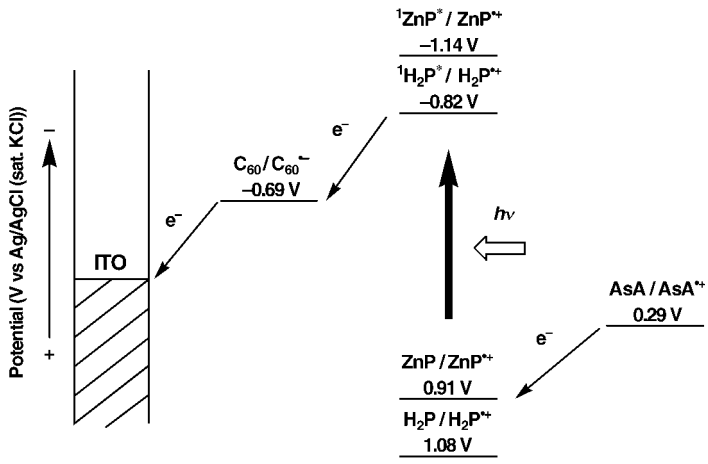

Scheme 4. Mechanism of photocurrent generation in dyad systems.

205 ps (19%)], which is in a good agreement with the fluorescence lifetimes of **Fc-ZnP-CONH-C_{60}**/ITO [53 ps (69%), 210 ps (31%)]. These results indicate the occurrence of photoinduced ET from the porphyrin excited singlet state to the C_{60} moiety on ITO.[42] Similar good matching between the fluorescence lifetimes [53 ps (92%), 420 ps (8%)] and the decay rate constants of transient absorbance at 430 nm [53 ps (46%), 300 ps (54%)] was found for **ZnP-CONH-C_{60}**/ITO (see Supporting Information S7).

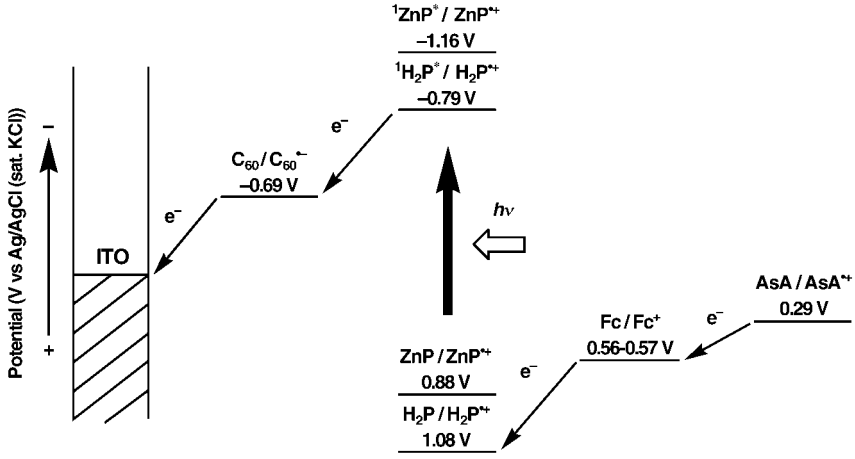

Scheme 5. Mechanism of photocurrent generation in triad systems.

Comparison of photoelectrochemical and photodynamic properties: Based on the above results together with the well-established photodynamics of porphyrin–fullerene linked systems on electrodes[16,17,27] and those of **Fc-P-CONH-C_{60}**, **P-CONH-C_{60}**, and **P-S1-C_{60}** in solution,[28] the mechanisms of photocurrent generation in Pt/AsA/**Fc-P-CONH-C_{60}**/ITO, Pt/AsA/**P-CONH-C_{60}**/ITO, and Pt/AsA/**P-S1-C_{60}**/ITO systems are summarized in Schemes 4 and 5. First, the mechanism of photocurrent generation of the dyad systems is presented for better understanding of the more complex triad systems. Intramolecular ET takes place from $^1P^*$ [H_2P: −0.82 V; ZnP: −1.14 V versus Ag/AgCl (saturated KCl)] to C_{60}, followed by intermolecular ET from AsA [+0.29 V versus Ag/AgCl (saturated KCl)] to porphyrin radical cation [H_2P: +1.08 V; ZnP: +0.91 V versus Ag/AgCl (saturated KCl)], yielding C_{60} radical anion ($C_{60}^{\bullet-}$) and AsA radical cation ($AsA^{\bullet+}$; Scheme 4). Photogenerated $C_{60}^{\bullet-}$ [−0.69 V versus Ag/AgCl (saturated KCl)] gives an electron to the ITO electrode, leading to anodic photocurrent generation. The quantum yields of CS of **ZnP-CONH-C_{60}** (99%)[28c] and **H_2P-CONH-C_{60}** (88%) in benzonitrile are much higher than that of **ZnP-S1-C_{60}** (18%) on the basis of results obtained by picosecond[29,43] and nanosecond transient absorption measurements (Figure 7 and Table 2). In the latter case, a stronger interaction between porphyrin and

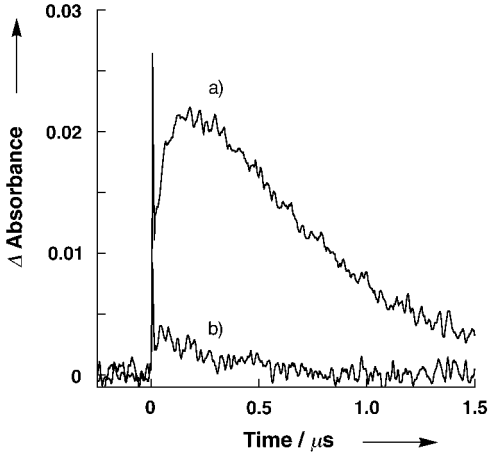

Figure 7. Time profiles of a) **ZnP-CONH-C_{60}** and b) **ZnP-S1-C_{60}** in benzonitrile at 1000 nm after photoexcitation at 530 nm.

fullerene for the charge-separated state of **ZnP-S1-C_{60}** results in the smaller quantum yield of CS, probably because of the rapid decay of the exciplex, formed initially by photoexitation, to the ground state rather than to the charge-separated state.[29,43,44] The initial absorption spike at 1000 nm observed in Figure 7 may correspond to the formation and decay of the exciplex state. The subsequent slow rise in absorbance at 1000 nm is ascribed to ET from the porphyrin moiety to the excited triplet state ($^3C_{60}^*$) and from the excited triplet state (^{3}ZnP*) to C_{60} to produce $C_{60}^{\bullet-}$ ($\lambda_{max}=$ 1000 nm), or conversion of the exciplex state to the CS state, followed by decay due to back-ET to the ground state. In the case of **ZnP-CONH-C_{60}**, weak interaction between porphyrin and fullerene for the CS state would result in a high quantum yield of CS, owing to the relatively rapid conversion of the exciplex state to the CS state rather than direct decay of the exciplex state to the ground state.[29,43,44] A large degree of delocalization within the three-dimensional framework of porphyrin and fullerene would stabilize the less polar exciplex state relative to the conventional donor–-acceptor linked systems to generate the exciplex state, even when the donor and the acceptor are linked by a relatively long spacer. The lifetimes of charge-separated states of **ZnP-CONH-C_{60}** (770 ns)[28] become longer than that of **H_2P-CONH-C_{60}** (45 ns).[28] This clearly demonstrates that the long-lived charge-separated state and the charge-separation efficiency are important controlling factors for achieving high quantum yields of photocurrent generation in donor–acceptor linked systems which are covalently attached to ITO surface. It is intriguing to compare the present photoelectrochemical systems with Pt/HV^{2+}/**C_{60}-NHCO-P**/ITO systems (P = ZnP or H_2P, HV^{2+} = hexylviologen),[27] in which the same porphyrin–fullerene dyads (i.e., **ZnP-CONH-C_{60}**) are covalently linked to the ITO surface in reverse order. The quantum yield of Pt/HV^{2+}/**C_{60}-NHCO-P**/ITO is 3.9%, which is smaller than that of Pt/AsA/**ZnP-CONH-C_{60}**/ITO (8.0%). This may result from the fact that the spacer between the ITO electrode and the porphyrin moiety in Pt/HV^{2+}/**C_{60}-NHCO-P**/ITO is longer than that between the ITO electrode and the C_{60} moiety in Pt/AsA/**ZnP-CONH-C_{60}**/ITO. In other words, a long spacer between the porphyrin moiety and the ITO electrode makes the ET rate constant small and results in poor photocurrent generation.

Taking into accounts the mechanism of photocurrent generation in porphyrin–fullerene dyad systems, the mechanism of photocurrent generation in ferrocene-porphyrin-fullerene triad systems shown in Scheme 5 is proposed. Intramolecular ET from ^{1}P* [H_2P: −0.79 V; ZnP: −1.16 V versus Ag/AgCl (saturated KCl)] to C_{60} is followed by intramolecular ET from ferrocene to porphyrin radical cation [H_2P: 1.08 V; ZnP: 0.88 V versus Ag/AgCl (saturated KCl)], to generate ferricenium ion (Fc^+) and the C_{60} radical anion ($C_{60}^{\bullet-}$). Intermolecular ET from AsA [+0.29 V versus Ag/AgCl (saturated KCl)] to Fc^+ ion [**Fc-ZnP-CONH-C_{60}**/ITO: 0.56 V; **Fc-H_2P-CONH-C_{60}**/ITO: 0.57 V versus Ag/AgCl (saturated KCl)] yields neutral ferrocene and AsA radical cation ($AsA^{\bullet+}$). Photogenerated $C_{60}^{\bullet-}$ [−0.69 V versus Ag/AgCl (saturated KCl)] gives an electron to the ITO electrode, leading to the anodic photocurrent generation. The quantum yields of CS of **Fc-ZnP-CONH-C_{60}** (99%),[28c] **ZnP-CONH-C_{60}** (99%),[28c] and **H_2P-CONH-C_{60}** (88%) in benzonitrile are much higher than that of **Fc-H_2P-CONH-C_{60}** (25%)[28c] on the basis of previous results. However, the lifetimes of the charge-separated states in benzonitrile are in the order of **H_2P-CONH-C_{60}** (45 ns)[28c] < **ZnP-CONH-C_{60}** (770 ns)[28c] < **Fc-ZnP-CONH-C_{60}** (7.7 μs)[28c] ≈ **Fc-H_2P-CONH-C_{60}** (8.3 μs).[28c] These results also reveal that long-lived charge-separated states and high charge-separation efficiency are responsible for realizing high quantum yields of photocurrent generation in donor–acceptor linked systems on ITO surface.

It is noteworthy that the highest internal quantum yield (11%) of photocurrent generation for the ITO electrodes is much lower than the efficiencies (20–25%) for gold electrodes with similar ferrocene–porphyrin–fullerene triads chemically attached to the surface.[16d,e] First, the structures of SAMs of the ferrocene–porphyrin–fullerene triads on the rough ITO surface is more complex than that on the atomically flat gold surface. In addition, a silane coupling reagent with three functional methoxyl groups usually polymerizes three-dimensionally with formation of complex structures. Such polymerization would make the surface modification with the triads complex. This may explain the low efficiency of photocurrent generation in the ITO electrode system. Thus, the internal quantum yield of photocurrent generation would be improved when donor–acceptor linked molecules exhibiting a high CS efficiency with a long lifetime are well-organized on the semiconductor electrode surface, which suppresses the energy-wasting EN quenching of the excited state of the sensitizers by the electrode surface.

Conclusion

We have successfully constructed systematic series of photoelectrochemical devices consisting of self-assembled monolayers of porphyrin–fullerene triads and dyads on ITO electrodes. The highest quantum yield of photocurrent generation (up to 11%) among donor–acceptor linked systems covalently attached to the surface of ITO electrodes was achieved with SAMs of ferrocene–zinc porphyrin–fullerene linked molecules on ITO electrodes. The mechanism of photocurrent generation was clarified by fluorescence lifetime measurements together with time-resolved transient absorption studies on the ITO systems. The quantum yields of photocurrent generation are well correlated with the charge-separation efficiency as well as the lifetime of the charge-separated state for ferrocene–porphyrin–fullerene triads and porphyrin–fullerene dyads in solution. These results provide valuable information for the construction of photonic molecular devices and artificial photosynthetic systems on ITO electrodes.

Experimental Section

General: Melting points were recorded on a Yanagimoto micro-melting apparatus and are not corrected. ^{1}H NMR spectra were measured on a JEOL EX-270. Matrix-assisted laser desorption/ionization (MALDI)

time of flight (TOF) mass spectra were measured on a Kratos Compact MALDI I (Shimadzu). UV/Vis spectra were obtained on a Shimadzu UV-3100 spectrometer. AFM measurements were performed in air in tapping mode using a NanoScope IIIa (Veeco metrology group/Digital Instruments). The roughness factor of the ITO surface ($R=1.3$) was determined by AFM measurements. All solvents and chemicals were of reagent grade, purchased commercially, and used without further purification unless otherwise noted. Tetrabutylammonium hexafluorophosphate used as a supporting electrolyte for the electrochemical measurements was obtained from Tokyo Kasei Organic Chemicals and recrystallized from methanol. Dry toluene and dry methylene chloride were heated to reflux and distilled from CaH_2. Thin-layer chromatography and flash column chromatography were performed with Alt. 5554 DC-Alufolien Kieselgel 60 F_{254} (Merck) and Fujisilica BW300, respectively. ITO electrodes (190–200 nm ITO on transparent glass slides) were obtained commercially from Evers, Inc. (Japan).

1a: A saturated solution of zinc acetate dihydrate in methanol (8 mL) was added to a solution of **1b**[28c] (64 mg, 50 μmol) in chloroform (50 mL) and refluxed for 5 h. After cooling, the reaction mixture was washed successively with a saturated aqueous solution of sodium bicarbonate and water, dried over anhydrous sodium sulfate, and then the solvent was removed under reduced pressure. **1a** was obtained as a deep purple solid from chloroform/methanol (64 mg, 47 μmol, 95% yield): m.p. > 300 °C; ^{1}H NMR ($CDCl_3$): $\delta=1.53$ (s, 36H), 4.10 (s, 5H), 4.35 (s, 2H), 4.69 (s, 2H), 7.58 (d, $J=7$ Hz, 2H), 7.75 (d, $J=7$ Hz, 2H), 7.82 (s, 2H), 8.02 (s, 4H), 8.09 (d, $J=2$ Hz, 4H), 8.13 (s, 1H), 8.28 (d, $J=7$ Hz, 2H), 8.29 (d, $J=7$ Hz, 2H), 8.33 (s, 1H), 8.38 (d, $J=7$ Hz, 2H), 8.40 (d, $J=7$ Hz, 2H), 8.91 (d, $J=5$ Hz, 2H), 8.94 (d, $J=5$ Hz, 2H), 9.04 (d, $J=5$ Hz, 2H), 10.02 ppm (s, 1H); MALDI-TOF MS (positive mode): m/z: 1352 [M+H$^+$].

2a: This compound was synthesized from **2b**[28b] by the same method as described for **1a**. (83% yield): m.p. > 300 °C; ^{1}H NMR ($CDCl_3$): $\delta=1.52$ (s, 54H), 7.79 (t, $J=8$ Hz, 2H), 8.00 (s, 4H), 8.08 (d, $J=2$ Hz, 2H), 8.09 (d, $J=2$ Hz, 4H), 8.26 (d, $J=8$ Hz, 2H), 8.33 (br s, 1H), 8.41 (d, $J=8$ Hz, 2H), 8.90 (d, $J=5$ Hz, 2H), 9.02 (s, 4H), 9.04 (d, $J=5$ Hz, 2H), 10.01 ppm (s, 1H); MALDI-TOF MS (positive mode): m/z: 1161 [M+H$^+$].

Cyclic voltammetry: All electrochemical studies were performed on a Bioanalytical Systems, Inc. CV-50W voltammetric analyzer using a standard three-electrode cell with a modified ITO working electrode (electrode area 0.48 cm^2), a platinum wire counterelectrode, and an Ag/AgCl (saturated KCl) reference electrode in CH_2Cl_2 containing 0.2 mol L^{-1} nBu$_4$NPF$_6$ as supporting electrolyte with a sweep rate of 0.10 V s^{-1}. The adsorbed amounts of compounds were determined from the charge of the anodic peak of the porphyrin first oxidation or the cathodic peak of the C_{60} first reduction.

Photoelectrochemical measurements: Photoelectrochemical measurements were performed in a one-compartment Pyrex UV cell (5 mL). The cell was illuminated with monochromatic excitation light through interference filters (MIF-S, Vacuum Optics Corporation of Japan) by a 180 W UV lamp (Sumida LS-140 V) or through a monochromator (Ritsu MC-10N) by a 500 W xenon lamp (Ushio XB-50101AA-A) on an SAM of area 0.48 cm^2. The photocurrent was measured in a three-electrode arrangement (Bioanalytical Systems, Inc. CV-50W) with a modified ITO working electrode (electrode area, 0.48 cm^2), a platinum wire counterelectrode (distance between electrodes 0.3 mm), and a Ag/AgCl (saturated KCl) reference electrode. The light intensity was monitored by an optical power meter (Anritsu ML9002A) and corrected. Internal quantum yields and IPCE values were calculated based on the number of photons absorbed by the chromophore and those incident photons on the ITO electrodes at each wavelength from the input power, the photocurrent density, and the absorbance determined from the absorption spectrum on the ITO electrode.

Fluorescence lifetime measurements: Fluorescence decays were measured by using femtosecond pulse laser excitation and a single-photon counting system for fluorescence decay measurements.[45] The laser system was a mode-locked Ti:sapphire laser (Coherent, Mira 900) pumped by an argon ion laser (Coherent, Innova 300). The repetition rate of laser pulses was 2.9 MHz with a pulse picker (Coherent, model 9200). The third harmonic generated by an ultrafast harmonic system (Inrad, model 5050) was used as excitation source. The excitation wavelength was set at 435 nm, and temporal profiles of fluorescence decay and rise were recorded with a microchannel plate photomultiplier (Hamamatsu R3809U). Full-width at half-maximum (fwhm) of the instrument response function was 36 ps when the time interval of the multichannel analyzer (CANBERRA, model 3501) was 2.6 ps in the channel number. Criteria for the best fit were the values of χ^2 and the Dubrin–Watson parameters, obtained by nonlinear regression.

Femtosecond transient absorption measurements: The dual-beam femtosecond time-resolved transient absorption spectrometer consisted of a self-mode-locked femtosecond Ti:sapphire laser (Coherent, MIRA), a Ti:sapphire regenerative amplifier (Clark MXR, CPA-1000) pumped by a Q-switched Nd:YAG laser (ORC-1000), a pulse stretcher/compressor, an optical parametric generation and optical parametric amplification (OPG-OPA) system, and an optical detection system.[46] A femtosecond Ti:sapphire oscillator pumped by a cw Nd:YVO4 laser (Coherent, Verdi) produced a train of 60 fs mode-locked pulses with an averaged power of 600 mW at 800 nm. The seed pulses from the oscillator were stretched (ca. 250 ps) and sent to a Ti:sapphire regenerative amplifier pumped by a Q-switched Nd:YAG laser operating at 1 kHz. The femtosecond seed pulses and Nd:YAG laser pulses were synchronized by adjusting an electronic delay between the Ti:sapphire oscillator and Nd:YAG laser. Then, the amplified pulse train inside the Ti:sapphire regenerative amplifier cavity was cavity-dumped by the Q-switching technique, and about 30000-fold amplification at 1 kHz was obtained. After recompression, the amplified pulses were color-tuned by OPG-OPA. The resulting laser pulses had a pulse width of about 150 fs and an average power of 5–30 mW at 1 kHz repetition rate in the range 550–700 nm. The pump beam was focused to a 1 mm diameter spot, and laser fluence was adjusted less than about 1.0 mJ cm^{-2} by using a variable neutral-density filter. The fundamental beam remaining in the OPG-OPA system was focused onto a flowing water cell to generate a white-light continuum, which was again split into two parts, one part of which was overlapped with the pump beam at the sample to probe the transient, while the other was passed through the sample without overlapping the pump beam. The time delay between pump and probe beams was controlled by making the pump beam travel along a variable optical delay. The white-light continuum beams after the sample were sent to a 15 cm focal length spectrograph (Acton Research) through each optical fiber and then detected by dual 512-channel photodiode arrays (Princeton Instruments). The intensity of the white light of each 512-channel photodiode array was processed to calculate the absorption difference spectrum at the desired time delay between pump and probe pulses. To obtain the time-resolved transient absorption difference signal at the specific wavelength, the monitoring wavelength was selected by using an interference filter. By chopping the pump pulses at 43 Hz, the modulated probe pulses and reference pulses were detected by two separate photodiodes. The output current was amplified with a homemade fast preamplifier, and then the resultant voltage signals of the probe pulses were gated and processed by a boxcar averager. The resultant modulated signal was measured by a lock-in amplifier and then fed into a PC for further signal processing.

Nanosecond transient absorption measurements: Nanosecond transient absorption measurements were carried with the SHG (530 nm) of an Nd:YAG laser (Spectra-Physics, Quanta-Ray GCR-130, fwhm 6 ns) as excitation source. For transient absorption spectra in the near-IR region (600–1600 nm), monitoring light from a pulsed Xe-lamp was detected with a Ge avalanche photodiode (Hamamatsu Photonics, B2834). Photoinduced events in nano- and microsecond time regimes were estimated by using a continuous Xe lamp (150 W) and an InGaAs PIN photodiode (Hamamatsu Photonics, G5125-10) as probe light and detector, respectively. Details of the transient absorption measurements are described elsewhere.[28c] All the samples (10^{-4} to 10^{-5} mol L^{-1}) in a quartz cell (1 × 1 cm) were deaerated by bubbling argon through the solution for 15 min.

Acknowledgement

This work was supported by the Development of Innovative Technology (No. 12310) from Ministry of Education, Culture, Sports, Science and Technology (MEXT), Japan. H.I. also thanks Grant-in-Aid from MEXT,

Japan (21st Century COE on Kyoto University Alliance for Chemistry) for financial support. The work at Yonsei University was supported by the National Creative Research Initiative Program of the Ministry of Science and Technology of Korea.

[1] a) M. R. Wasielewski, *Chem. Rev.* **1992**, *92*, 435; b) R. A. Marcus, *Angew. Chem.* **1993**, *105*, 1161; *Angew. Chem. Int. Ed. Engl.* **1993**, *32*, 1111; c) M. Bixon, J. Jortner, *Adv. Chem. Phys.* **1999**, *106*, 35; d) D. Gust, T. A. Moore in *The Porphyrin Handbook*, *Vol. 8* (Eds.: K. M. Kadish, K. M. Smith, R. Guilard), Academic Press, San Diego, **2000**, pp. 153 – 190; e) V. Balzani, *Electron Transfer in Chemistry*, Wiley-VCH, Weinheim, **2001**.

[2] a) H. Imahori, Y. Sakata, *Adv. Mater.* **1997**, *9*, 537; b) H. Imahori, Y. Sakata, *Eur. J. Org. Chem.* **1999**, 2445; c) H. Imahori, Y. Mori, Y. Matano, *J. Photochem. Photobiol. C* **2003**, *4*, 51; d) D. M. Guldi, *Chem. Commun.* **2000**, 321; e) H. Imahori, S. Fukuzumi, *Adv. Funct. Mater.* **2004**, *14*, 525; f) H. Imahori, *J. Phys. Chem. B* **2004**, *108*, 6130; g) H. Imahori, *Org. Biomol. Chem.* **2004**, *2*, 1425.

[3] a) H. Imahori, K. Hagiwara, T. Akiyama, M. Aoki, S. Taniguchi, T. Okada, M. Shirakawa, Y. Sakata, *Chem. Phys. Lett.* **1996**, *263*, 545; b) H. Imahori, N. V. Tkachenko, V. Vehmanen, K. Tamaki, H. Lemmetyinen, Y. Sakata, S. Fukuzumi, *J. Phys. Chem. A* **2001**, *105*, 1750; c) H. Imahori, H. Yamada, D. M. Guldi, Y. Endo, A. Shimomura, S. Kundu, K. Yamada, T. Okada, Y. Sakata, S. Fukuzumi, *Angew. Chem.* **2002**, *114*, 2450; *Angew. Chem. Int. Ed.* **2002**, *41*, 2344.

[4] a) A. Ulman, *An Introduction to Ultrathin Organic Films*, Academic Press, San Diego, **1991**; b) J. Jortner, M. A. Ratner, *Molecular Electronics*, Blackwell, Oxford, **1997**; c) C. A. Mirkin, *Inorg. Chem.* **2000**, *39*, 2258; d) A. N. Shipway, E. Katz, I. Willner, *ChemPhysChem* **2000**, *1*, 18; e) A. P. Alivisatos, P. F. Barbara, A. W. Castleman, J. Chang, D. A. Dixon, M. L. Klein, G. L. McLendon, J. S. Miller, M. A. Ratner, P. J. Rossky, S. I. Stupp, M. E. Thompson, *Adv. Mater.* **1998**, *10*, 1297.

[5] a) C. A. Mirkin, W. B. Caldwell, *Tetrahedron* **1996**, *52*, 5113; b) X. Shi, W. B. Caldwell, K. Chen, C. A. Mirkin, *J. Am. Chem. Soc.* **1994**, *116*, 11598; c) W. B. Caldwell, K. Chen, C. A. Mirkin, S. J. Babinec, *Langmuir* **1993**, *9*, 1945; d) Y.-S. Shon, K. F. Kelly, N. J. Halas, T. R. Lee, *Langmuir* **1999**, *15*, 5329; e) T. Hatano, A. Ikeda, T. Akiyama, S. Yamada, M. Sano, Y. Kanekiyo, S. Shinkai, *J. Chem. Soc. Perkin Trans. 2* **2000**, *5*, 909.

[6] a) F. Arias, L. A. Godínez, S. R. Wilson, A. E. Kaifer, L. Echegoyen, *J. Am. Chem. Soc.* **1996**, *118*, 6086; b) O. Domínguez, L. Echegoyen, F. Cunha, N. Tao, *Langmuir* **1998**, *14*, 821; c) L. Echegoyen, L. E. Echegoyen, *Acc. Chem. Res.* **1998**, *31*, 593; d) S.-G. Liu, C. Martineau, J.-M. Raimundo, J. Roncali, L. Echegoyen, *Chem. Commun.* **2001**, 913.

[7] H. Imahori, T. Azuma, A. Ajavakom, H. Norieda, H. Yamada, Y. Sakata, *J. Phys. Chem. B* **1999**, *103*, 7233.

[8] a) M. Lahav, T. Gabriel, A. N. Shipway, I. Willner, *J. Am. Chem. Soc.* **1999**, *121*, 258; b) M. Lahav, V. Heleg-Shabtai, J. Wasserman, E. Katz, I. Willner, H. Dürr, Y.-Z. Hu, S. H. Bossmann, *J. Am. Chem. Soc.* **2000**, *122*, 11480; c) K. Uosaki, T. Kondo, X.-Q. Zhang, M. Yanagida, *J. Am. Chem. Soc.* **1997**, *119*, 8367; d) T. Kondo, M. Yanagida, S.-I. Nomura, T. Ito, K. Uosaki, *J. Electroanal. Chem.* **1997**, *438*, 121; e) F. B. Abdelrazzaq, R. C. Kwong, M. E. Thompson, *J. Am. Chem. Soc.* **2002**, *124*, 4796.

[9] a) E. Katz, I. Willner, *Langmuir* **1997**, *13*, 3364; b) J. Zak, H. Yuan, M. Ho, L. K. Woo, M. D. Porter, *Langmuir* **1993**, *9*, 2772; c) J. E. Hutchison, T. A. Postlethwaite, C.-H. Chen, K. W. Hathcock, R. S. Ingram, W. Ou, R. W. Linton, R. W. Murray, D. A. Tyvoll, L. L. Chng, J. P. Collman, *Langmuir* **1997**, *13*, 2143; d) J. E. Hutchison, T. A. Postlethwaite, R. W. Murray, *Langmuir* **1993**, *9*, 3277; e) T. R. E. Simpson, D. J. Revell, M. J. Cook, D. A. Russell, *Langmuir* **1997**, *13*, 460; f) D. T. Gryko, F. Zhao, A. A. Yasseri, K. M. Roth, D. F. Bocian, W. G. Kuhr, J. S. Lindsey, *J. Org. Chem.* **2000**, *65*, 7356.

[10] a) G. Ashkenasy, G. Kalyuzhny, J. Libman, I. Rubinstein, A. Shanzer, *Angew. Chem.* **1999**, *111*, 1333; *Angew. Chem. Int. Ed.* **1999**, *38*, 1257; b) N. Kanayama, T. Kanbara, H. Kitano, *J. Phys. Chem. B* **2000**, *104*, 271; c) D. A. Offord, S. B. Sachs, M. S. Ennis, T. A. Eberspacher, J. H. Griffin, C. E. D. Chidsey, J. P. Collman, *J. Am. Chem. Soc.* **1998**, *120*, 4478; d) I. Willner, V. Heleg-Shabtai, E. Katz, H. K. Rau, W. Haehnel, *J. Am. Chem. Soc.* **1999**, *121*, 6455; e) E. Soto, J. C. MacDonald, G. F. C. Cooper, W. G. McGimpsey, *J. Am. Chem. Soc.* **2003**, *125*, 2838.

[11] a) S. Fukuzumi, H. Imahori in *Electron Transfer in Chemistry*, *Vol. 2* (Ed.: V. Balzani), Wiley-VCH, Weinheim, **2001**, pp. 927 – 975; b) H. Imahori, H. Norieda, S. Ozawa, K. Ushida, H. Yamada, T. Azuma, K. Tamaki, Y. Sakata, *Langmuir* **1998**, *14*, 5335; c) H. Imahori, H. Norieda, Y. Nishimura, I. Yamazaki, K. Higuchi, N. Kato, T. Motohiro, H. Yamada, K. Tamaki, M. Arimura, Y. Sakata, *J. Phys. Chem. B* **2000**, *104*, 1253.

[12] a) J. J. Hickman, D. Ofer, C. Zou, M. S. Wrighton, P. E. Laibinis, G. M. Whitesides, *J. Am. Chem. Soc.* **1991**, *113*, 1128; b) C. D. Frisbie, J. R. Martin, R. R. Duff, Jr., M. S. Wrighton, *J. Am. Chem. Soc.* **1992**, *114*, 7142; c) S. Creager, C. J. Yu, C. Bamdad, S. O'Connor, T. MacLean, E. Lam, Y. Chong, G. T. Olsen, J. Luo, M. Gozin, J. F. Kayyem, *J. Am. Chem. Soc.* **1999**, *121*, 1059; d) T. Kondo, S. Horiuchi, I. Yagi, S. Ye, K. Uosaki, *J. Am. Chem. Soc.* **1999**, *121*, 391; e) H. Byrd, E. P. Suponeva, A. B. Bocarsly, M. E. Thompson, *Nature* **1996**, *380*, 610.

[13] a) W. B. Caldwell, D. J. Campbell, K. Chen, B. R. Herr, C. A. Mirkin, A. Malik, M. K. Durbin, P. Dutta, K. G. Huang, *J. Am. Chem. Soc.* **1995**, *117*, 6071; b) D. J. Campbell, B. R. Herr, J. C. Hulteen, R. P. Van Duyne, C. A. Mirkin, *J. Am. Chem. Soc.* **1996**, *118*, 10211; c) D. G. Walter, D. J. Campbell, C. A. Mirkin, *J. Phys. Chem. B* **1999**, *103*, 402.

[14] a) I. Willner, *Acc. Chem. Res.* **1997**, *30*, 347; b) R. Blonder, S. Levi, G. Tao, I. Ben-Dov, I. Willner, *J. Am. Chem. Soc.* **1997**, *119*, 10467; c) A. Doron, M. Portnoy, M. Lion-Dagan, E. Katz, I. Willner, *J. Am. Chem. Soc.* **1996**, *118*, 8937; d) T. Morita, S. Kimura, S. Kobayashi, Y. Imanishi, *J. Am. Chem. Soc.* **2000**, *122*, 2850; e) K. M. Roth, J. S. Lindsey, D. F. Bocian, W. G. Kuhr, *Langmuir* **2002**, *18*, 4030.

[15] a) M. A. Fox, *Acc. Chem. Res.* **1999**, *32*, 201; b) M. O. Wolf, M. A. Fox, *J. Am. Chem. Soc.* **1995**, *117*, 1845; c) M. O. Wolf, M. A. Fox, *Langmuir* **1996**, *12*, 955; d) M. A. Fox, M. D. Wooten, *Langmuir* **1997**, *13*, 7099; e) W. Li, V. Lynch, H. Thompson, M. A. Fox, *J. Am. Chem. Soc.* **1997**, *119*, 7211; f) S. Reese, M. A. Fox, *J. Phys. Chem. B* **1998**, *102*, 9820.

[16] a) T. Akiyama, H. Imahori, A. Ajavakom, Y. Sakata, *Chem. Lett.* **1996**, 907; b) H. Imahori, S. Ozawa, K. Ushida, M. Takahashi, T. Azuma, A. Ajavakom, T. Akiyama, M. Hasegawa, S. Taniguchi, T. Okada, Y. Sakata, *Bull. Chem. Soc. Jpn.* **1999**, *72*, 485; c) H. Imahori, H. Yamada, S. Ozawa, K. Ushida, Y. Sakata, *Chem. Commun.* **1999**, 1165; d) H. Imahori, H. Yamada, Y. Nishimura, I. Yamazaki, Y. Sakata, *J. Phys. Chem. B* **2000**, *104*, 2099; e) H. Imahori, H. Norieda, H. Yamada, Y. Nishimura, I. Yamazaki, Y. Sakata, S. Fukuzumi *J. Am. Chem. Soc.* **2001**, *123*, 100.

[17] a) H. Imahori, Y. Nishimura, H. Norieda, H. Karita, I. Yamazaki, Y. Sakata, S. Fukuumi, *Chem. Commun.* **2000**, 661; b) H. Imahori, T. Hasobe, H. Yamada, Y. Nishimura, I. Yamazaki, S. Fukuzumi, *Langmuir* **2001**, *17*, 4925; c) T. Morita, S. Kimura, S. Kobayashi, Y. Imanishi, *Chem. Lett.* **2000**, 676; d) H. Imahori, S. Fukuzumi, *Adv. Mater.* **2001**, *13*, 1197.

[18] R. W. Murray, *Molecular Design of Electrode Surfaces*, Wiley, New York, **1992**, pp. 1 – 48.

[19] Organic solar cells containing films of donor-linked fullerenes on ITO: a) J.-F. Eckert, J.-F. Nicoud, J.-F. Nierengarten, S.-G. Liu, L. Echegoyen, F. Barigelletti, N. Armaroli, L. Ouali, V. Krasnikov, G. Hadziioannou, *J. Am. Chem. Soc.* **2000**, *122*, 7467; b) T. Gu, D. Tsamouras, C. Melzer, V. Krasnikov, J.-P. Gisselbrecht, M. Gross, G. Hadziioannou, J.-F. Nierengarten, *ChemPhysChem* **2002**, *3*, 124; c) J.-F. Nierengarten, J.-F. Eckert, J.-F. Nicoud, L. Ouali, V. Krasnikov, G. Hadziioannou, *Chem. Commun.* **1999**, 617; d) E. Peeters, P. A. van Hal, J. Knol, C. J. Brabec, N. S. Sariciftci, J. C. Hummelen, R. A. J. Janssen, *J. Phys. Chem. B* **2000**, *104*, 10174.

[20] Photoactive SAMs on ITO were reported to generate photocurrent: a) A. Ikeda, T. Hatano, S. Shinkai, T. Akiyama, S. Yamada, *J. Am. Chem. Soc.* **2001**, *123*, 4855; b) T.-X. Wei, J. Zhai, J.-H. Ge, L.-B. Gan, C.-H. Huang, G.-B. Luo, L.-M. Ying, T.-T. Liu, X.-S. Zhao, *Appl. Surf. Sci.* **1999**, *151*, 153; c) H. Yamada, H. Imahori, Y. Nishimura, I. Yamazaki, S. Fukuzumi, *Chem. Commun.* **2000**, 1921; d) T.

Hasobe, H. Imahori, H. Yamada, T. Sato, K. Ohkubo, S. Fukuzumi, *Nano Lett.* **2003**, *3*, 409; e) H. Imahori, K. Hosomizu, Y. Mori, T. Sato, T. K. Ahn, S. K. Kim, D. Kim, Y. Nishimura, I. Yamazaki, H. Ishii, H. Hotta, Y. Matano, *J. Phys. Chem. B* **2004**, *108*, 5018.

[21] SAMs of photoactive single chromophores on other metal oxides (SnO_2 and TiO_2) exhibited photocurrent generation: a) T. Osa, M. Fujihira, *Nature* **1976**, *264*, 349; b) M. Fujihira, N. Ohishi, T. Osa, *Nature* **1977**, *268*, 226; c) S. Anderson, E. C. Constable, M. P. Dare-Edwards, J. B. Goodenough, A. Hamnett, K. R. Seddon, R. D. Wright, *Nature* **1979**, *280*, 571; d) M. A. Fox, F. J. Nobes, T. A. Voynick, *J. Am. Chem. Soc.* **1980**, *102*, 4036; e) A. Hagfeldt, M. Grätzel, *Acc. Chem. Res.* **2000**, *33*, 269.

[22] SAMs of donor–acceptor dyad systems on nanoparticulate semiconductors (TiO_2) were reported to generate photocurrent: a) R. Argazzi, C. A. Bignozzi, T. A. Heimer, F. N. Castellano, G. J. Meyer, *J. Am. Chem. Soc.* **1995**, *117*, 11815; b) P. Bonhôte, J.-E. Moser, R. Humphry-Baker, N. Vlachopoulos, S. M. Zakeeruddin, L. Walder, M. Grätzel, *J. Am. Chem. Soc.* **1999**, *121*, 1324; c) C. J. Kleverlaan, M. T. Indelli, C. A. Bignozzi, L. Pavanin, F. Scandola, G. M. Hasselman, G. J. Meyer, *J. Am. Chem. Soc.* **2000**, *122*, 2840; d) P. V. Kamat, S. Barazzouk, S. Hotchandani, K. G. Thomas, *Chem. Eur. J.* **2000**, *6*, 3914; e) C. A. Bignozzi, R. Argazzi, C. J. Kleverlaan, *Chem. Soc. Rev.* **2000**, *29*, 87; f) *Molecular Level Artificial Photosynthetic Materials* (Ed.: G. J. Meyer), Wiley, New York, **1997**; g) N, Hirata, J.-J. Lagref, E. J. Palomares, J. R. Durrant, M. K. Nazeeruddin, M. Grätzel, D. D. Censo, *Chem. Eur. J.* **2004**, *10*, 595.

[23] Vectorial photoinduced ET of donor–acceptor dyads in Langmuir–Blodgett (LB) films on ITO was observed: a) N. V. Tkachenko, E. Vuorimaa, T. Kesti, A. S. Alekseev, A. Y. Tauber, P. H. Hynninen, H. Lemmetyinen, *J. Phys. Chem. B* **2000**, *104*, 6371; b) A. S. Alekseev, N. V. Tkachenko, A. Y. Tauber, P. H. Hynninen, R. Osterbacka, H. Stubb, H. Lemmetyinen, *J. Phys. Chem. B* **2002**, *275*, 243; c) N. V. Tkachenko, A. Y. Tauber, P. H. Hynninen, A. Y. Sharonov, H. Lemmetyinen, *J. Phys. Chem. A* **1999**, *103*, 3657.

[24] Layer-by-layer noncovalent deposition of ruthenium complex–C_{60} dyad on ITO was reported for the fabrication of photoactive films exhibiting photocurrent generation: C. Luo, D. M. Guldi, M. Maggini, E. Menna, S. Mondini, N. A. Kotov, M. Prato, *Angew. Chem.* **2000**, *112*, 4052; *Angew. Chem. Int. Ed.* **2000**, *39*, 3905.

[25] For application of electrophoretically deposited metal nanoclusters covered with photoactive chromophores on optically transparent electrodes in the photoelectrochemical conversion of light energy, see: a) P. K. Sudeep, B. I. Ipe, K. G. Thomas, M. V. George, S. Barazzouk, S. Hotchandani, P. V. Kamat, *Nano Lett.* **2002**, *2*, 29; b) P. V. Kamat, S. Barazzouk, K. G. Thomas, S. Hotchandani, *J. Phys. Chem. B* **2000**, *104*, 4014; c) P. V. Kamat, *J. Phys. Chem. B* **2002**, *106*, 7729; d) T. Hasobe, H. Imahori, P. V. Kamat, S. Fukuzumi, *J. Am. Chem. Soc.* **2003**, *125*, 14962.

[26] K. Chen, W. B. Caldwell, C. A. Mirkin, *J. Am. Chem. Soc.* **1993**, *115*, 1193.

[27] a) H. Yamada, H. Imahori, Y. Nishimura, I. Yamazaki, S. Fukuzumi, *Adv. Mater.* **2002**, *14*, 892; b) H. Yamada, H. Imahori, Y. Nishimura, I. Yamazaki, T. K. Ahn, S. K. Kim, D. Kim, S. Fukuzumi, *J. Am. Chem. Soc.* **2003**, *125*, 9129.

[28] a) H. Imahori, M. E. El-Khouly, M. Fujitsuka, O. Ito, Y. Sakata, S. Fukuzumi, *J. Phys. Chem. A* **2001**, *105*, 325; b) C. Luo, D. M. Guldi, H. Imahori, K. Tamaki, Y. Sakata, *J. Am. Chem. Soc.* **2000**, *122*, 6535; c) H. Imahori, K. Tamaki, D. M. Guldi, C. Luo, M. Fujitsuka, O. Ito, Y. Sakata, S. Fukuzumi, *J. Am. Chem. Soc.* **2001**, *123*, 2607.

[29] a) T. J. Kesti, N. V. Tkachenko, V. Vehmanen, H. Yamada, H. Imahori, S. Fukuzumi, H. Lemmetyinen, *J. Am. Chem. Soc.* **2002**, *124*, 8067; b) N. V. Tkachenko, H. Lemmetyinen, J. Sonoda, K. Ohkubo, T. Sato, H. Imahori, S. Fukuzumi, *J. Phys. Chem. A* **2003**, *107*, 8834.

[30] D. Hammel, C. Kautz, K. Müllen, *Chem. Ber.* **1990**, *123*, 1353.

[31] a) M. Maggini, G. Scorrano, M. Prato, *J. Am. Chem. Soc.* **1993**, *115*, 9798; b) M. Prato, M. Maggini, *Acc. Chem. Res.* **1998**, *31*, 519.

[32] K. Kordatos, S. Bosi, T. Da Ros, A. Zambon, V. Lucchini, M. Prato, *J. Org. Chem.* **1996**, *61*, 4764.

[33] The regioselectivity of bis-adducts could not be determined because of the complex molecular structures on the ITO surface.

[34] The red shift and broadening of the Soret band of SAMs of porphyrins on gold surfaces were reported to be due to the partially stacked side-by-side porphyrin aggregation (i.e., J aggregation) in the SAMs;[11c] see: R. F. Khairutdinov, N. Serpone, *J. Phys. Chem. B* **1999**, *103*, 761.

[35] The reduction wave due to the C_{60} moiety was irreversible. It is known that fullerenes exhibit no reversible electrochemical response when they are embedded in films: N. Nakashima, T. Ishii, M. Shirakusa, T. Nakanishi, H. Murakami, T. Sagara, *Chem. Eur. J.* **2001**, *7*, 1766.

[36] The reduction wave due to the C_{60} moiety was not reproducible when the C_{60} moiety attached to the ITO surface was further modified with porphyrin or ferrocene-porphyrin molecules.[35] The reduction potential due to the C_{60} moiety may be shifted in negative direction (by ca. 200 mV) because of possible bis-addition.[31,32]

[37] Synthetic porphyrin dimers in close proximity generally exhibit a negative shift in oxidation potential due to interaction between the porphyrins.[11c,16d] On the other hand, the decreased dielectric constant in the nonpolar monolayers as compared to that in bulk solution results in a positive shift in oxidation potential of the porphyrin. Such compensation may be responsible for a small difference in oxidation potential of the porphyrins in monolayers and in solution.[11c,16d]

[38] AsA may form a complex with the porphyrin moiety of the SAMs on the ITO electrode when the electron transfer rate from AsA to the ferrocene moiety becomes independent of AsA concentration. Similar complex formation is seen when methylviolgen or hexylviologen is used as an electron carrier in electrolyte solution in the photoelectrochemical system of porphyrin SAMs[17b] or porphyrin-modified gold nanoclusters in benzonitrile; see: S. Fukuzumi, Y. Endo, Y. Kashiwagi, Y. Araki, O. Ito, H. Imahori, *J. Phys. Chem. B* **2003**, *107*, 11979.

[39] The fluorescence lifetime of **ZnP-S1-C_{60}** in benzonitrile is reported to be about 1 ps.[29] Since the time resolution of the fluorescence lifetime measurements on the ITO system is about 2 ps, a minor decay process of the porphyrin excited singlet state may be involved in the fluorescence lifetimes of **ZnP-S1-C_{60}**/ITO under the present experimental conditions.

[40] The short fluorescence lifetimes of **P-ref**/ITO (P = ZnP or H_2P) relative to **P-ref** in solution (ca. 2 ns for **ZnP-ref** and ca. 10 ns for **H_2P-ref**) result from self-quenching of the porphyrin excited singlet state due to aggregation on ITO.

[41] The fluorescence lifetime of similar porphyrin–fullerene dyads incorporated in LB systems is known to be short relative to that in solution. Accelerated photoinduced ET is suggested in the LB film: N. V. Tkachenko, V. Vehmanen, J.-P. Nikkanen, H. Yamada, H. Imahori, S. Fukuzumi, H. Lemmetyinen, *Chem. Phys. Lett.* **2002**, *366*, 245.

[42] Characteristic absorption due to ZnP radical cation (around 660 nm) and C_{60} radical anion (around 1000 nm) could not be confirmed because of poor signal-to-noise ratio. The input laser power was minimized to avoid exciton–exciton annihilation processes, which occur dominantly within a few picoseconds after laser excitation, especially at high power.

[43] N. V. Tkachenko, L. Rantala, A. Y. Tauber, J. Helaja, P. H. Hynninen, H. Lemmetyinen, *J. Am. Chem. Soc.* **1999**, *121*, 9378.

[44] The high quantum yield of photocurrent generation in Pt/AsA/**H_2P-S1-C_{60}**/ITO (3.4%) relative to Pt/AsA/**ZnP-S1-C_{60}**/ITO (1.7%) may result from differences in the photodynamics of **H_2P-S1-C_{60}** and **ZnP-S1-C_{60}** and the complexation of porphyrin with AsA.[38] Photoexcitation of **H_2P-S1-C_{60}** in benzonitrile results in formation of the CS state, whereas photoexcitation of **ZnP-S1-C_{60}** in benzonitrile leads to the initial formation of the exciplex followed by the CS state.[29] Similar photoelectrochemical behavior was observed for analogous photoelectrochemical systems of porphyrin–fullerene dyads on gold electrodes.[16b]

[45] a) N. Boens, N. Tamai, I. Yamazaki, T. Yamazaki, *Photochem. Photobiol.* **1990**, *52*, 911; b) Y. Nishimura, A. Yasuda, S. Speiser, I. Yamazaki, *Chem. Phys. Lett.* **2000**, *323*, 117.

[46] H. S. Cho, N. W. Song, Y. H. Kim, S. C. Jeoung, S. Hahn, D. Kim, S. K. Kim, N. Yoshida, A. Osuka, *J. Phys. Chem. A* **2000**, *104*, 3287.

Received: April 20, 2004
Published online: August 27, 2004

